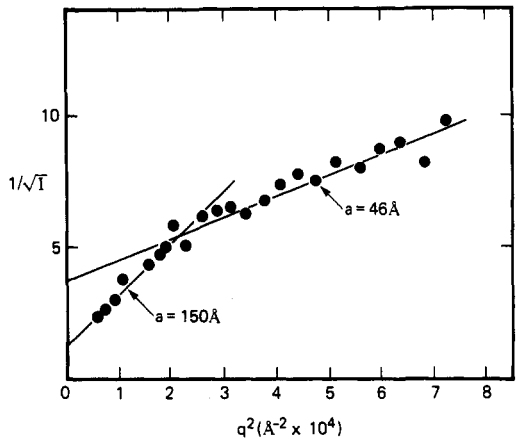


**Figure 2.** Plot of $I^{-1/2}$ vs. $q^2$ for PIB/PMMA particles doped with 0.5% $(C_65H_5)_4Pb$ and suspended in an ethanol/water mixture. The data plotted are those in excess of thermal density fluctuation scattering.

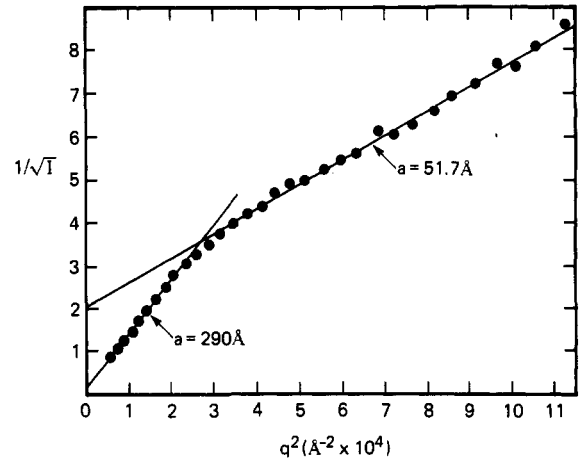


**Figure 3.** Plot of $I^{-1/2}$ vs. $q^2$ for PIB/PMMA particles doped with 1% $(C_6H_5)_4Pb$ and suspended in an ethanol/water mixture.

pure PIB. This, however, is not correct since grafting between the PMMA and PIB chains would lead to a diffuse interface between the phases. It is clear though that small-angle X-ray scattering shows evidence of the formation of microphases and, in fact, two different size scales are observed. What is not clear, at present, is the precise meaning of these size scales.

Up to this point, attention has been focused on the angular dependence of the scattering, and, as shown in eq 4, the mean square fluctuation of the election density difference should provide information on the actual densities of the phases giving rise to the observed scattering. While measurements were performed on an absolute level, evaluation of the electron density difference between the phases was not reliable for several reasons. First, it is necessary to know the volume fractions of the phases giving rise to the scattering. This, as mentioned before, is not possible with any degree of precision. Second, it is clear from the results presented that the phases are not monodisperse in size and a significant proportion of the scattering occurs at scattering angles that are not accessible experimentally. Thus, the total integrated scattering from which $\overline{(\Delta\eta)^2}$ is obtained would be low due to truncation effects. Finally, it would be necessary to assume that the distribution of the $(C_6H_5)_4Pb$ in the PIB phase is uniform and that the extent of penetration of the $(C_6H_5)_4Pb$ into the PIB is small. Thus, while measurement of the total integrated scattering could yield, in principle, the electron density difference between the individual phases, too many assumptions and restrictions were encountered to make even qualitative use of this quantity.

In conclusion, small-angle scattering measurements on PIB-stabilized PMMA particles doped with $(C_6H_5)_4Pb$ show clearly that there are microphase-separated regions within the particles. This is consistent with our previous hypothesis.[4] The size scales of the heterogeneities are consistent with our previous fluorescence energy-transfer studies in further support of our model.

**Registry No.** (IB)(MMA) (copolymer), 30971-07-4.

## References and Notes

(1) For review, see: (a) Winnik, M. A. *Polym. Eng. Sci.* **1983**, *24*, 87–97; (b) Winnik, M. A. *Pure Appl. Chem.* **1984**, 56, 1281–1288.
(2) Pekcan, O.; Winnik, M. A.; Croucher, M. D. *J. Colloid Interface Sci.* **1983**, *95*, 420–427.
(3) Pekcan, O.; Winnik, M. A.; Egan, L. S.; Croucher, M. D. *Macromolecules* **1983**, *16*, 699–702.
(4) Pekcan, O.; Winnik, M. A.; Croucher, M. D. *J. Polym. Sci., Polym. Lett. Ed.* **1983**, *21*, 1011–1018.
(5) Sperling, L. H. *Polym. Eng. Sci.* **1985**, *25*, 517–520.
(6) Berens, A. R.; Hopfenberg, H. B. *J. Membr. Sci.* **1982**, *10*, 283.
(7) Debye, P.; Bueche, A. M. *J. Appl. Phys.* **1940**, *20*, 518.
(8) Debye, P.; Anderson, H. R.; Brumberger, H. *J. Appl. Phys.* **1957**, *28*, 679.
(9) Kratky, O. *J. Pure. Appl. Chem.* **1966**, *12*, 483.

# Communications to the Editor

## Monolayer Polymerization of Methyl 2-(Octadecanamido)propenoate: An Amphiphilic Captodative Monomer Based on Dehydroalanine

We recently began exploring the polymerizability of a new family of dehydroalanine monomers 1 available in high yield from DL-serine.[1] The common dehydroalanine structure offers enormous potential as a basic building block for functional polymers. First, it offers *two* sites for derivatization: a carboxyl moiety capable of existing as a free acid, carboxylate anion, and a wide range of ester and amide derivatives; and an enamine nitrogen which may be converted to a host of amide or amine derivatives. Second, dehydroalanines are unusually active in free radical polymerizations. In our work, for example, one sample of the decanamide derivative (1, $n$ = 8) spontaneously formed polymer of over 15 million molecular weight.[1]

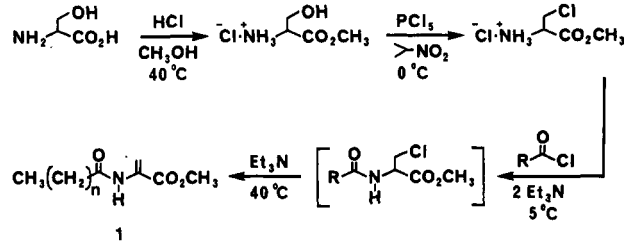


1

Captodative stabilization of the propagating radical

0024-9297/87/2220-0901$01.50/0 

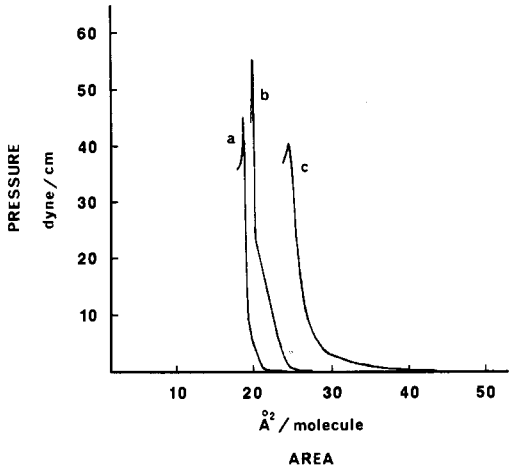


**Figure 1.** Pressure vs. area curves for (a) methyl stearate, (b) stearic acid (pH = 2), and (c) monomer 1 at 20.2 °C at the air/water (pH = 5.6) interface.

offers one explanation for such behavior; i.e., the nitrogen lone pair electrons offer donor (dative) stabilization while the carbonyl provides (capto) resonance stabilization involving the C=O bond:[2]

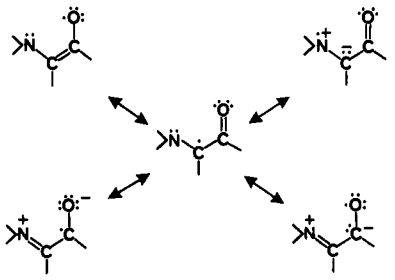

Our goal in synthesizing the long-alkyl derivatives of 1 was to examine their potential to form and polymerize in organized structures such as monolayers and vesicles. We report here initial results confirming monolayer polymerization of the stearic acid derivative (1, $n$ = 16).

*Experimental.* Stearoyl chloride (Aldrich) and 3-chloroalanine methyl ester hydrochloride[1] were reacted in cold benzene using triethylamine (Aldrich) as base on a 50-mmol scale in quantitative yield. The monomer was recrystallized three times from hexanes, mp 53.6–54.5 °C, and was analytically pure by GLC.

Poly(methyl 2-(octadecanamide)propenoate) was obtained by free radical polymerization of a 10% solution in hexanes at 60 °C with Vazo-67 initiator (Du Pont). Polymer was purified by precipitation from THF into methanol and drying under high vacuum; $[\eta]$ = 1.59 dL/g, $\bar{M}_w = 1.72 \times 10^6$ by LALLS (both at 25 °C in THF).

All monolayer experiments were performed on a thermostated Lauda Langmuir film balance (Messgerate-Werk Lauda, FRG) using degassed, deionized water. Carefully weighed aliquots of the standards or stearamide monomer were dissolved in hexane (Alfa, 99+%) to give $10^{-3}$ M solutions. Compression began 15 min after deposition and all experiments (compression and expansion) were run at a specific rate of 3 Å$^2$ molecule$^{-1}$ min$^{-1}$ on a bulk water subphase temperature of 20.2 ± 0.5 °C, with a relative humidity of 55–65%.

Polymerizations required a nitrogen atmosphere and water purged with nitrogen prior to use as the subphase. The monomer film was held under constant pressure for 155–260 s until the change in area over time was less than 2.1 cm$^2$/min. The film was then exposed to two 15-W UV lamps (Sylvania germicidal) positioned 8 cm above the gas/water interface. The barrier was then expanded to its maximum area. After 5 min the monolayer was compressed and expanded to obtain the surface pressure vs. area curves. Three replicate polymerizations were carried out at each constant pressure while monitoring area change. Polymer identity was confirmed by $^1$H NMR and FTIR, with the latter carried out on as-obtained thin films using an ATR cell and as a KBr pellet.

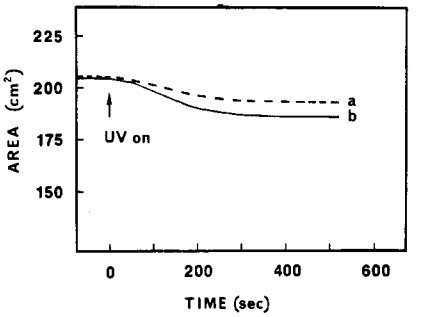


**Figure 2.** Area vs. time plot of UV-initiated polymerization of monomer held at (a) 12 dyn/cm and (b) 25 dyn/cm constant pressure.

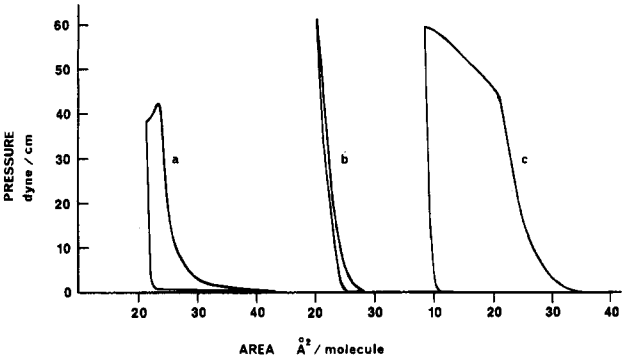


**Figure 3.** Pressure vs. area curves for (a) monomer 1, (b) UV-polymerized monolayer, and (c) free radical polymer.

*Results and Discussion.* Monolayer pressure–area isotherms recorded for monomer 1, steric acid, and methyl stearate are shown in Figure 1. Average values for the area per molecule at collapse were 23.6 ± 0.1, 19.3 ± 0.4, and 17.7 ± 0.7 Å$^2$, respectively, with associated collapse pressures of 41.0 ± 1.2, 55.2 ± 1.0, and 45.1 ± 0.9 dyn/cm. Values for the standards compared well with published values.[3-5]

Figure 2 gives typical curves obtained for polymerizations at constant pressures of 12 and 25 dyn/cm. Each shows an induction period of 75 and 66 s, respectively. The initial rapid decrease in area leveled off at 380–460 s. Relative rates of the initial linear portions of the graphs (ca. 150 s) were compared. The rate at 25 dyn/cm was found to be 1.6 times greater than that at 12 dyn/cm. This rate increase is consistent with an increase in orientation due to the closer packing of the monolayer at the higher pressure. Intermolecular amide hydrogen bonding may also contribute to the orientation of the monomer at the gas/water interface.

Initial confirmation of polymer formation was obtained from the differences in the $\pi$–$A$ curve for the monolayer-polymerized product compared to monomer and solution-polymerized material (Figure 3). Most important was the increase in the sharpness of the compression transition and collapse pressure (>60 dyn/cm$^2$) for the monolayer polymer compared to monomer. The curve for a prepolymerized sample shows a broad pressure increase with a compression transition (change in slope) at 21 Å$^2$ similar to monomer but very different from the in situ polymerized monolayer. Similar results have been ob-

tained by others in the polymerization of monomers in monolayers.[6,7]

We conclude that well-behaved monolayers are formed from this monomer and that UV-initiated polymerization takes place to give greatly stabilized and less compressable monolayer products containing polymer and residual monomer.

**Acknowledgment.** We gratefully acknowledge continued financial support for this project from 3M and helpful discussions with Dr. J. K. Rasmussen of 3M's Corporate Research Laboratory.

**Registry No.** 1, 106133-27-1; 1 (homopolymer), 106158-81-0.

## References and Notes

(1) Mathias, L. J.; Hermes, R. E. *Macromolecules* **1986**, *19*, 1536–1542.
(2) Viehe, H. G.; Janousek, Z.; Merenyi, R.; Stella, L. *Acc. Chem. Res.* **1985**, *18*, 148–154.
(3) Gaines, G. L., Jr. *Insoluble Monolayers at Liquid–Gas Interfaces*; Wiley: New York, 1966.
(4) Demchak, R. J.; Fort, T., Jr. *J. Colloid Interface Sci.* **1974**, *46*, 191.
(5) Sackmann, H.; Dorfler, H. D. *Z. Phys. Chem. (Leipzig)* **1972**, *251*, 303.
(6) O'Brian, K. C.; Long, J.; Lando, J. B. *Langmuir* **1985**, *1*, 514.
(7) Laschewsky, A.; Ringsdorf, H.; Schmidt, G.; Schneider, J. *J. Am. Chem. Soc.* **1986**, *109*, 788–796.

**Robert E. Hermes and Lon J. Mathias***
*Department of Polymer Science*
*University of Southern Mississippi*
*Hattiesburg, Mississippi 39406*

**Judson W. Virden, Jr.**
*Science Research Laboratory, 3M Center*
*St. Paul, Minnesota 55144*

*Received December 9, 1986*

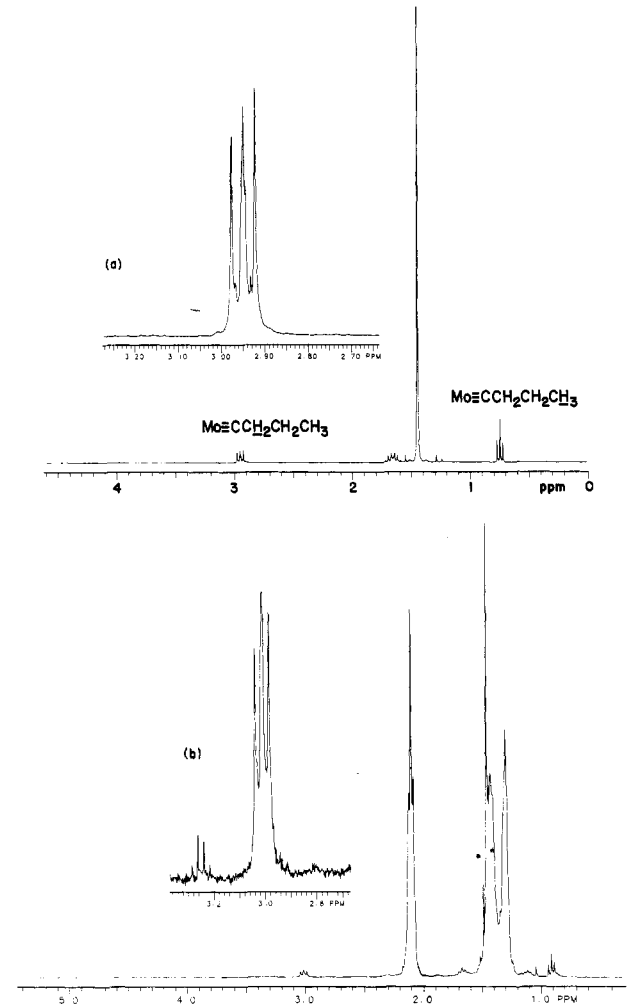


**Figure 1.** (a) $^1$H NMR spectrum of (a)Mo($CCH_2CH_2CH_3$)-($OCMe_3$)$_3$ in $C_6D_6$; (b) $^1$H NMR spectrum of Mo{[C-($CH_2$)$_6$C]$_x$CPr}($OCMe_3$)$_3$ prepared by adding 15 equiv of cyclooctyne to the sample of Mo(CPr)($OCMe_3$)$_3$.

## Ring-Opening Polymerization of Cyclooctyne

The ring-opening polymerization of cyclic olefins by olefin metathesis catalysts is now well-known,[1] and well-characterized catalysts are being discovered that allow one to prepare living polymers of this type.[2] Acetylene metathesis catalysts also are now well characterized.[3] The fact that their reactivity also can be altered greatly by the choice of metal (Mo or W) and the nature of the alkoxide ligand system created the possibility that an acetylene metathesis catalyst could be designed that would polymerize cyclooctyne (ring strain ~9 kcal mol$^{-1}$) by metathetical ring opening to give a living polymer. We report here a successful system of this type.

Acetylene metathesis catalysts that are highly active for the metathesis of internal acetylenes (e.g., W(CR)($O^tBu$)$_3$[3a]) are not suitable for the controlled ring opening of cyclooctyne since the alkylidyne also will react with triple bonds in the growing chain. However, catalysts that are much less active are obtained simply by changing the metal from W to Mo.[3d] In fact, Mo($C^tBu$)($O^tBu$)$_3$ will not react with 3-heptyne, although it will react rapidly with 1-pentyne (eq 1).[3d] Mo(CPr)($O^tBu$)$_3$ (**1a**) reacts only very slowly with

$$\mathrm{Mo(C^tBu)(O^tBu)_3 + PrC{\equiv}CH \rightarrow Mo(CPr)(O^tBu)_3 + {^t}BuC{\equiv}CH} \quad (1)$$

3-heptyne over several hours at 25 °C in benzene or toluene. The most characteristic features in the $^1$H NMR spectrum of Mo(CPr)($O^tBu$)$_3$ in $C_6D_6$ (Figure 1a) are signals for the Mo≡C$CH_2CH_2CH_3$ protons at 2.95 ppm and the Mo≡C$CH_2CH_2CH_3$ protons at 0.74 ppm. Upon addition of 15 equiv of cyclooctyne these signals disappear and are replaced by those characteristic of what we believe to be Mo{[C($CH_2$)$_6$C]$_x$CPr}($O^tBu$)$_3$ (**1b**, Figure 1b); the Mo≡C$CH_2$R signal can be seen clearly at 3.02 ppm and the signal for the methyl group in the propyl cap at 0.92 ppm. The $^{13}$C NMR spectrum (in $C_6D_6$) of the product made with 20 equiv of cyclooctyne exhibits a resonance at 80.4 ppm (among other expected resonances) that is shifted significantly from that for cyclooctyne at 94.5 ppm.[4] The range of chemical shifts for acetylenic carbon atoms in linear acetylenes is 75–90 ppm, while the range of chemical shifts for olefinic carbon atoms is 100–145 ppm. On this basis we contend that a ring opening has occurred, rather than formation of a polyene.

If only 1–5 equiv of cyclooctyne are added to Mo(CPr)($O^tBu$)$_3$, all of the cyclooctyne is consumed, but not all of **1a** is converted into **1b**, and the relative amounts of **1a** and **1b** vary from one experiment to another. The failure to convert all of **1a** into **1b** could be due either to a fast reaction between cyclooctyne and **1a** relative to the rate of mixing or to a slower rate of reaction of cyclooctyne with **1a** than with **1b**. The latter would be surprising; **1a** was chosen as the initiator precisely so that it would react with cyclooctyne as rapidly as the propagating species **1b**. The former also is more consistent with different initial ratios of **1a** to **1b** being observed.

Over a period of 24 h the ratio of **1a** to **1b** slowly changes to reach what we believe to be equilibrium values (Table

0024-9297/87/2220-0903$01.50/0 